Research Square

Preprints are preliminary reports that have not undergone peer review.
They should not be considered conclusive, used to inform clinical practice,
or referenced by the media as validated information.

Numerical simulations of inorganic HTL- free perovskite Cs 2 PtI 6 solar cell using SCAPS-1D

Hadeer H. AbdElAziz

hadeer.hesham@psas.bsu.edu.eg

Faculty of Postgraduate Studies for Advanced Sciences (PSAS)

Waleed M.A. El Rouby

Faculty of Postgraduate Studies for Advanced Sciences (PSAS)

M. H. Khedr

Faculty of Postgraduate Studies for Advanced Sciences (PSAS)

Laila Saad

Faculty of Postgraduate Studies for Advanced Sciences (PSAS)

Research Article

Keywords:

Posted Date: March 10th, 2026

DOI: https://doi.org/10.21203/rs.3.rs-8914352/v1

License: This work is licensed under a Creative Commons Attribution 4.0 International License.
Read Full License

Additional Declarations: No competing interests reported.

Abstract

This study utilizes the SCAPS-1D to conduct a numerical simulation of lead-free solar cell device based on Cs_2PtI_6. We aim to explore the impact of eliminating hole transport materials (HTL) on the device's performance while ensuring high efficiency and stability. The investigated device structure includes FTO/CdS/Cs_2PtI_6 with a back metal electrode, along with several performance variants. Our findings reveal that the HTL-free Cs_2PtI_6 solar cell maintains a power conversion efficiency (PCE) of 20.3% under solar illumination. Additionally, we perform parametric studies examining how variations in absorber layer thickness, doping density, and metal back contacts influence the solar cell's PCE.

1. Introduction

The energy crisis problem is spreading around the world because of the limitation of fuel energy resources and the bad environmental effects from burning fuels. Perovskite materials are considered as emerging materials for solar cell devices. Perovskites have outstanding electronic and optical properties to make high efficiency solar cell devices. Perovskite is named after the minerologist Perovski who discovered these materials. Perovskite structure has the chemical formula of ABX_3 where A and B are metallic cations and X is halide for solar cell applications. The first prototype synthesized perovskite solar cell achieved a PCE of 3.8 in 2009 using $CH_3NH_3PbI_3$ material [1]. The PCE of perovskite solar cell devices increased until it reached up to 26.1%, recently [2]. However, the perovskite solar cell-based devices have a high PCE, they suffer from two main problems. First, organic cation A is degradable which has a bad effect on device stability. Second, the toxic cation B lead (Pb^+). The organic cation A can be replaced by inorganic cations like Cesium (Cs^+) or Rubidium (Rb^+) or Potassium (K^+). One of the well-studied perovskite material is $CsPbI_3$ [3],[4],[5] and has a PCE of around 21.53%, recently [6]. $CsPbI_3$ is considered as a wide bandgap semiconductor material with a bandgap of 1.7 eV and contains toxic Pb element. Another inorganic perovskite material is $CsSnI_3$ has a bandgap of ~ 1.3 eV which meets the criteria for capturing most of solar light [7]. On the other hand, $CsSnI_3$ material suffers from instability because of the Sn^{+2} element that oxidizes fast to Sn^{+4} and forms the Cs_2SnI_6 compound [8]. The Cs_2SnI_6 based solar cell device has an efficiency of 1.5% and the mixed halide $Cs_2SnI_2Br_4$ achieves a PCE of 2.025% only [9],[10]. These challenges direct the research to find stable lead-free perovskite material. One of the derived perovskite materials is the vacancy ordered A_2BX_6. Cs_2PtI_6 crystalizes in the form of Fm3m K_2PtCl_6 cubic structure form [11]. It has an optical band gap of ~ 1.4 eV which is suitable semiconductor material for capturing solar spectrum. In ambient conditions, the stability of Cs_2PtI_6 material reaches one year [12], [13]. The material has a defect density of $2.5X10^{12}$ cm^{-3} and a 2 µs lifetime carrier. A prototype of Cs_2PtI_6 perovskite solar cell device a PCE of 13.88% using ethylene diamine treatment [13]. Cs_2PtI_6 is also used as a photo anode for photo-electro chemical water oxidation process [14],[15] for its stability in acidic environment. The n-i-p planar perovskite solar cell device structure consists of a glass layer like fluorine tin oxide (FTO), or indium tin oxide (ITO) followed by electron transport layer (ETL). The next layer is the perovskite layer followed by the hole transport layer

(HTL) and back electrode. ETL materials should meet the criteria of high chemical, photostability and electron mobility to facilitate electrons transport. HTL materials have an important role in the perovskite solar cell device. HTL material facilitates the hole extraction of the perovskite to the electrode and ban electrons from moving to the anode [16]. Thus, it increases device efficiency. Spiro-OMeTAD material is widely used as an efficient HTL material in perovskite solar cell devices. On the other hand, Spiro-OMeTAD degraded fast as it is organic material and is expensive [17]. The challenge is to produce HTL-free perovskite solar cell device while maintaining high efficiency. In this study, the Cs_2PtI_6 material is simulated as the main absorber layer of solar cell. We investigated the effect of removing HTL material layer on the PCE of the device by numerical analysis using one dimensional solar cell capacitance simulation program (SCAPS-1D) [18], [19]. SCAPS-1D simulator works by solving the semiconductor Poisson and continuity equations for specific boundary conditions. SCAPS-1D accepts up to 7 layers of materials and the simulation is performed by entering the material parameters of each layer. CdS is used as the ETL materials for the simulation to verify the experimental results and it has good bandgap alignment with Cs_2PtI_6. The effect of metal back contact electrode material (like C, Au, Pd, Pt, Se) on PCE is studied. Other parameters that affect the PCE of solar cells like Cs_2PtI_6 thickness, concentration doping, and defect density are studied. Table S1 (supporting information) lists the previous studies of Cs_2PtI_6- based solar cell device structures and parameters. Till date, there is a single experimental study of Cs_2PtI_6 based solar cell device with PCE of 10% with CdS as ETL and Spiro-OMeTAD as HTL [13]. The other studies concentrate on the numerical simulation of the device with the choice of different ETL and HTL materials. The highest PCE of Cs_2PtI_6 solar cell device is achieved with a structure of ($FTO/SnS_2/Cs_2PtI_6/MoTe_2/Au$) ~ 33%. To our best knowledge, till date there is no numerical analysis of HTL-free Cs_2PtI_6 based perovskite solar cell device.

2. The Simulated Structure

Table S2 (supporting information) lists the properties of materials used in this simulation study. The data are collected from previous experimental and numerical research studies. The front contact is modeled by flat bands. The back electrode is varied by different metals like carbon C work function = 5 eV, gold Au work function = 5.1 eV, palladium Pd work function = 5.6 eV, platinum work function = 5.7 eV [20], [21]. The series resistance Rs = 14 Ω. Front interface defect layer (IDL) between ETL and perovskite is used. IDL is modeled like perovskite absorber layer with small thickness ~ 5 nm. For Cs_2PtI_6 active layer, the thermal velocity of electrons and holes is 10^7 cm/s. The capture cross section of electrons and holes are estimated to be $2X10^{-14}$ cm^2. A neutral defect distribution with different concentrations for every material N_t is used. The defect density is calculated as follows: -

$$N_t = \frac{1}{\sigma \ \tau \ V_{th}}$$

Where V_{th} is the thermal velocity of carriers, τ is the carrier lifetime and σ is the capture cross section of electrons and holes. The τ value of Cs_2PtI_6 is > 2 μs, then the estimated N_t of Cs_2PtI_6 is

$2.5X10^{12}$ cm^{-3}.

Figure 1 (a) shows the band gap alignment of the HTL-free Cs_2PtI_6 perovskite solar cell device structure. The simulation structure consists of FTO layer followed by an ETL, perovskite layer, and metal back contact as shown in Fig. 1(b).

3. Results and Discussion

3.1. Variation of Metal Contacts

To investigate the impact of different metal contacts on the performance of the simulated solar cell device (FTO/CdS/Cs_2PtI_6/metal contact), four materials were analyzed, each with distinct work functions: carbon (C) at approximately 5 eV, gold (Au) at around 5.1 eV, palladium (Pd) at roughly 5.6 eV, and platinum (Pt) at about 5.7 eV. As illustrated in Fig. 2 (a), the J-V characteristics of the HTL-free Cs_2PtI_6 perovskite solar cell reveal that the lowest short-circuit current (Jsc) and open-circuit voltage (Voc) occur with the carbon back contact. An increase in work function correlates with enhanced Voc values, with the optimal performance achieved using Pt as the metal back contact. The power conversion efficiency (PCE) of the structure FTO/CdS/Cs_2PtI_6/metal contact rises from 4.4% with carbon to 14.1% with Pt.

3.2. Active Layer Thickness of Cs_2PtI_6

The thickness of the absorber layer significantly influences solar cell performance. While a thicker semiconductor layer allows for greater light absorption, it can also lead to increased carrier recombination, adversely affecting PCE. Consequently, optimizing layer thickness is crucial for device efficiency. The thickness of Cs_2PtI_6 varied from 200 nm to 800 nm. Numerical analysis of the J-V characteristics (Figure a) shows that as the thickness of Cs_2PtI_6 increases, the current density rises due to improved light absorption. However, at 800 nm thickness, the current density levels off, indicating high carrier recombination rates that negatively impact PCE. Figure (b) displays the quantum efficiency (QE) of the device at different Cs_2PtI_6 thicknesses, showing that greater thickness leads to enhanced photon absorption and QE. In terms of PCE, Fig. 3 (c) indicates a gradual increase from 14.1% at 200 nm to 15.75% at 600 nm thickness, followed by a slight decrease to 15.65% at 800 nm. The optimal thickness for Cs_2PtI_6 is thus determined to be 600 nm.

3.3. Doping Concentration of Cs_2PtI_6

Carrier density in the active material is critical for solar cell performance. Increasing doping density generates a stronger electric field, enhancing carrier separation and current generation. However, excessive doping can reduce the depletion region of the semiconductor and compress the electric field at the interface with the electron transport layer (ETL), hindering carrier collection and ultimately

lowering current density. Therefore, it is essential to optimize the doping concentration (N_A) of Cs_2PtI_6, varying it from 10^{16} to 10^{22} cm^{-3}. As shown in Fig. 4 (a), the J-V characteristics of FTO/CdS/ Cs_2PtI_6 (600 nm)/Pt reveal that both J and V values increase with higher N_A until a notable decline in Jsc occurs at 10^{22} cm^{-3}. Figure 4 (b) shows that the optimal PCE is achieved with an N_A of 10^{20} cm^{-3}.

3.5 Optimized structure

From the numerical analysis of the HTL-free Cs_2PtI_6 perovskite solar cell, the optimized structure is identified as FTO/CdS/Cs_2PtI_6 (600 nm)/Pt. This configuration achieves high performance with an acceptor doping concentration of 10^{20} cm^{-3} and a defect density of 10^{12} cm^{-3}. Figure S1(a) (supporting information) presents the J-V characteristics of the optimized device, which exhibits a Voc of 1.25 V, a short-circuit current of 28.2 mA/cm², a fill factor of 59.3%, and a PCE of 20.3%. The optimized solar cell demonstrates excellent absorption across the solar spectrum, particularly in the visible and near-infrared regions, as shown in Figure S1(b) (supporting information).

Conclusion

This study employs a SCAPS-1D numerical simulation to evaluate the performance of an HTL-free Cs_2PtI_6-based perovskite solar cell with a structure of FTO/CdS/Cs_2PtI_6/metal contact. The incorporation of a platinum metal contact significantly enhances the PCE of the solar cell. A parametric analysis was conducted on the Cs_2PtI_6 active layer concerning thickness, doping concentration, and defect density to optimize PCE. The maximum PCE achieved with the structure FTO/CdS/Cs_2PtI_6/Pt is 20.3% at a thickness of 600 nm, a doping concentration of 10^{20} cm^{-3}, and a defect density of 10^{12} cm^{-3}. The findings provide valuable insights for the design of a fully inorganic, lead-free, stable perovskite solar cell.

Declarations

Acknowledgements

The authors would like to thank Prof. Dr. Marc Burgelman, University of Gent, Belgium, for providing the SCAPS-1D simulation software.

Author contribution statement

Hadeer H. AbdElAziz:

Performed the simulations; Analyzed and interpreted the data; Wrote the paper.

Waleed M.A. El Rouby and M.H. Khedr:

Conceived and designed the experiments; Analyzed and interpreted the data.

Laila Saad

Contributed in choosing materials, analysis tools or data; Revised the paper.

Funding statement

This research did not receive any specific grant from funding agencies in the public, commercial, or not-for-profit sectors.

Data availability statement

All data are included in the article.

The authors declare no conflict of interest

Consent to Publish declaration: not applicable

Consent to Participate declaration: not applicable

Ethics declaration: not applicable

References

1. Kojima A, Teshima K, Shirai Y, Miyasaka T. Organometal Halide Perovskites as Visible-Light Sensitizers for Photovoltaic Cells. J Am Chem Soc. May 2009;131(17):6050–1. 10.1021/ja809598r.
2. Green MA, et al. Solar cell efficiency tables (Version 64). Prog Photovoltaics Res Appl. 2024;32:425–41. 10.1002/pip.3831.
3. Shi J, Wang Y, Zhao Y. Inorganic CsPbI3 Perovskites toward High-Efficiency Photovoltaics. Energy Environ Mater. 2019;2(2):73–8. 10.1002/eem2.12039.
4. Lin L et al. December., Simulated development and optimized performance of CsPbI3 based all-inorganic perovskite solar cells, *Sol. Energy*, vol. 198, no. 2019, pp. 454–460, 2020. 10.1016/j.solener.2020.01.081
5. AbdelAziz HH. Performance evaluation of free hole-transport layer CsPbI3 perovskite solar cells. J Mater Sci Mater Electron. 2023;34(6):0–11. 10.1007/s10854-022-09624-5.
6. Li T et al. Ambient Air Processed Inverted Inorganic Perovskite Solar Cells with over 21% Efficiency Enabled by Multifunctional Ethacridine Lactate. Angew Chemie, p. e202407508, 2024.
7. Wu B, et al. Long Minority-Carrier Diffusion Length and Low Surface-Recombination Velocity in Inorganic Lead-Free CsSnI3 Perovskite Crystal for Solar Cells. Adv Funct Mater. 2017;27(7). 10.1002/adfm.201604818.
8. Qiu X, et al. From unstable CsSnI3 to air-stable Cs2SnI6: A lead-free perovskite solar cell light absorber with bandgap of 1.48 eV and high absorption coefficient. Sol Energy Mater Sol Cells. 2017;159:227–34. 10.1016/j.solmat.2016.09.022.

9. Lee B, Krenselewski A, Il Baik S, Seidman DN, Chang RPH. Solution processing of air-stable molecular semiconducting iodosalts, Cs2SnI6-xBrx, for potential solar cell applications. Sustain Energy Fuels. 2017;1(4):710–24. 10.1039/c7se00100b.
10. Ullah S, et al. Lead-Free Cs2SnI6 Perovskites for Optoelectronic Applications: Recent Developments and Perspectives. Sol RRL. 2021;5:1–26. 10.1002/solr.202000830.
11. Kristallstrukturen E, Hexaiodoplatinates O, Pti IVM. Über Hexaiodoplatinate(IV) M 2 PtI 6 (M = K, Rb, Cs, NH 4, Tl) - Darstellungsverfahren, Eigenschaften und Kristallstrukturen. Z für Naturforsch B. 1983;38(8):905–10.
12. Yang S, Wang L, Zhao S, Liu A, Zhou Y, Han Q. Supporting Information A novel Lead-free material Cs 2 PtI 6 with Narrow Bandgap and Ultra-stable for Its Photovoltaic Application, pp. 4–8.
13. Schwartz D, et al. Air Stable, High-Efficiency, Pt-Based Halide Perovskite Solar Cells with Long Carrier Lifetimes. Phys Status Solidi - Rapid Res Lett. 2020;14(8):1–8. 10.1002/pssr.202000182.
14. Jayaraman JP, Hamdan M, Velpula M, Kaisare NS, Chandiran AK. BiVO4/Cs2PtI6 Vacancy-Ordered Halide Perovskite Heterojunction for Panchromatic Light Harvesting and Enhanced Charge Separation in Photoelectrochemical Water Oxidation, *ACS Appl. Mater. Interfaces*, vol. 13, no. 14, pp. 16267–16278, Apr. 2021, 10.1021/acsami.0c22654
15. Hamdan M, Chandiran AK. Cs2PtI6 Halide Perovskite is Stable to Air, Moisture, and Extreme pH: Application to Photoelectrochemical Solar Water Oxidation. Angew Chemie - Int Ed. 2020;59(37):16033–8. 10.1002/anie.202000175.
16. Li S, Cao YL, Li WH, Bo ZS. A brief review of hole transporting materials commonly used in perovskite solar cells. Rare Met. 2021;40(10):2712–29. 10.1007/s12598-020-01691-z.
17. Rombach FM, Haque SA, Macdonald TJ. Lessons learned from spiro-OMeTAD and PTAA in perovskite solar cells. Energy Environ Sci. 2021;14(10):5161–90. 10.1039/d1ee02095a.
18. Burgelman M, Nollet P, Degrave S. Modelling polycrystalline semiconductor solar cells. Thin Solid Films. 2000;361:527–32. 10.1016/S0040-6090(99)00825-1.
19. Burgelman M, Decock K, Kheli S, Abass A. Advanced electrical simulation of thin film solar cells. Thin Solid Films. 2013;535:296–301.
20. Behrouznejad F, Shahbazi S, Taghavinia N, Wu HP, Wei-Guang Diau E. A study on utilizing different metals as the back contact of CH3NH3PbI3 perovskite solar cells. J Mater Chem A. 2016;4(35):13488–98. 10.1039/c6ta05938d.
21. Deepthi Jayan K, Sebastian V. Comprehensive device modelling and performance analysis of MASnI3 based perovskite solar cells with diverse ETM, HTM and back metal contacts, *Sol. Energy*, vol. 217, no. February, pp. 40–48, 2021, 10.1016/j.solener.2021.01.058

Figures

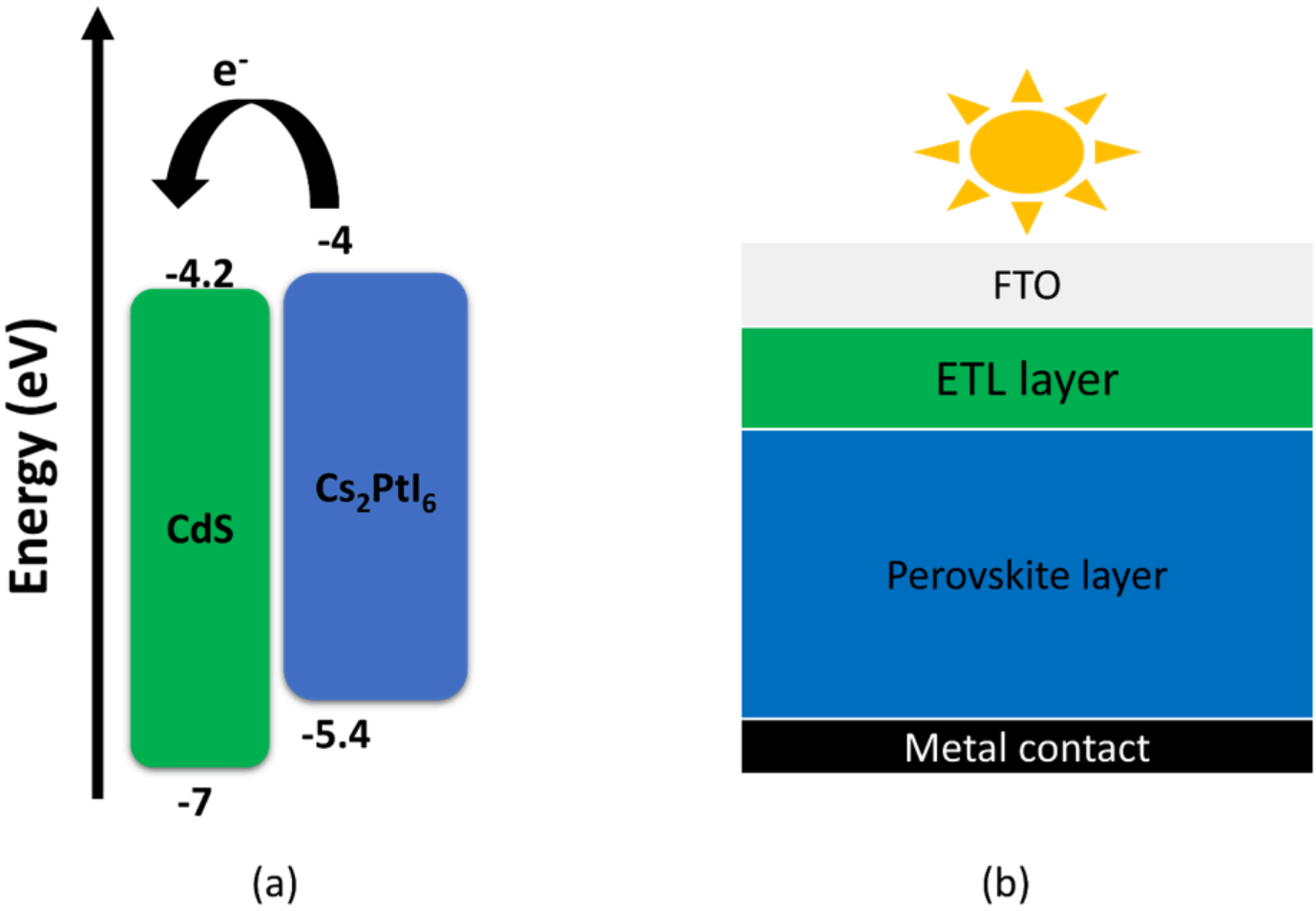

Figure 1

(a) Bandgap alignment of CdS/Cs_2PtI_6 (b) Proposed HTL-free solar cell device structure (FTO/CdS/Cs_2PtI_6/metal contact)

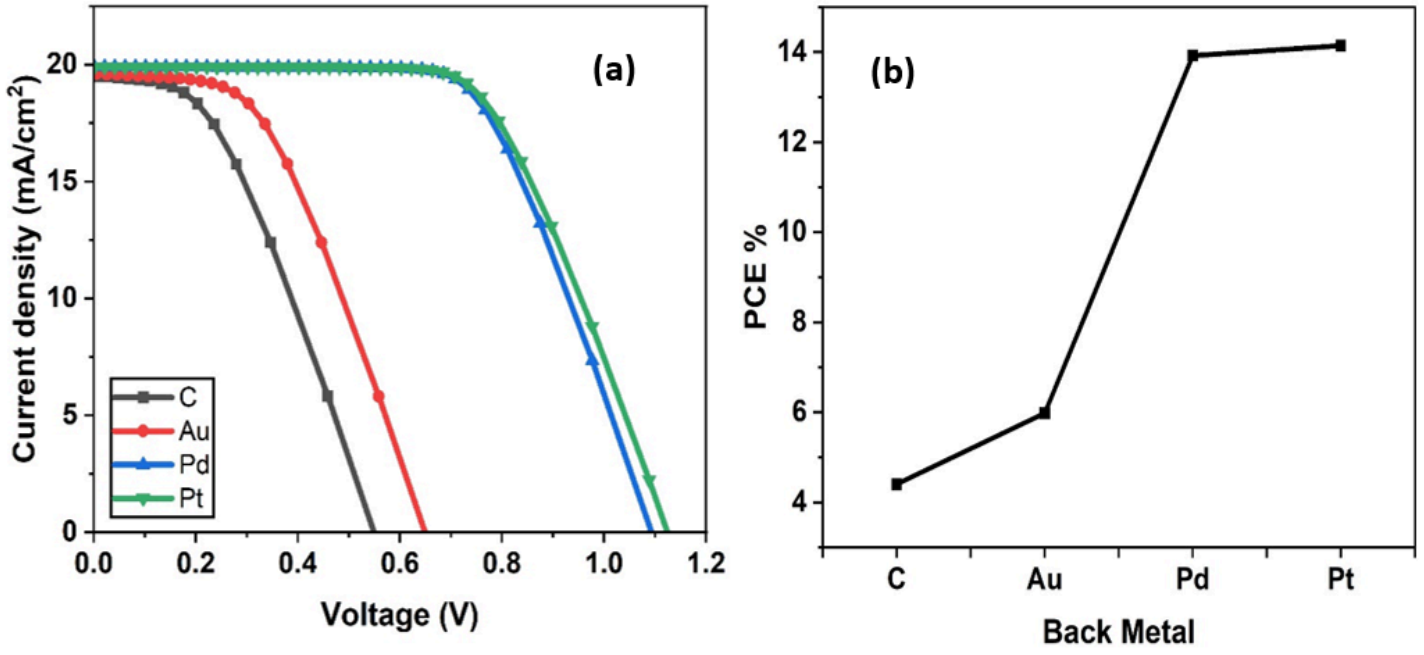

Figure 2

(a) J-V diagram of FTO/ETL/Cs_2PtI_6/back metal, (b) PCE

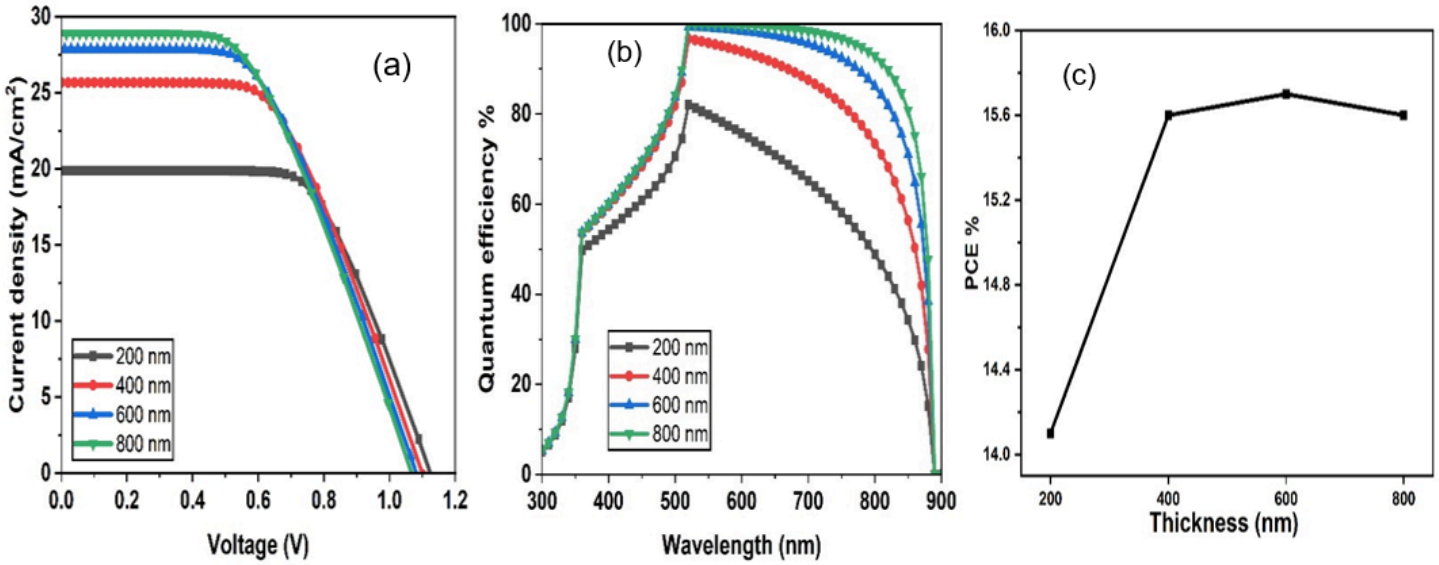

Figure 3

The numerical analysis of FTO/Cs_2PtI_6(different thickness)/Pt based solar cell device (a) J-V diagram, (b) QE

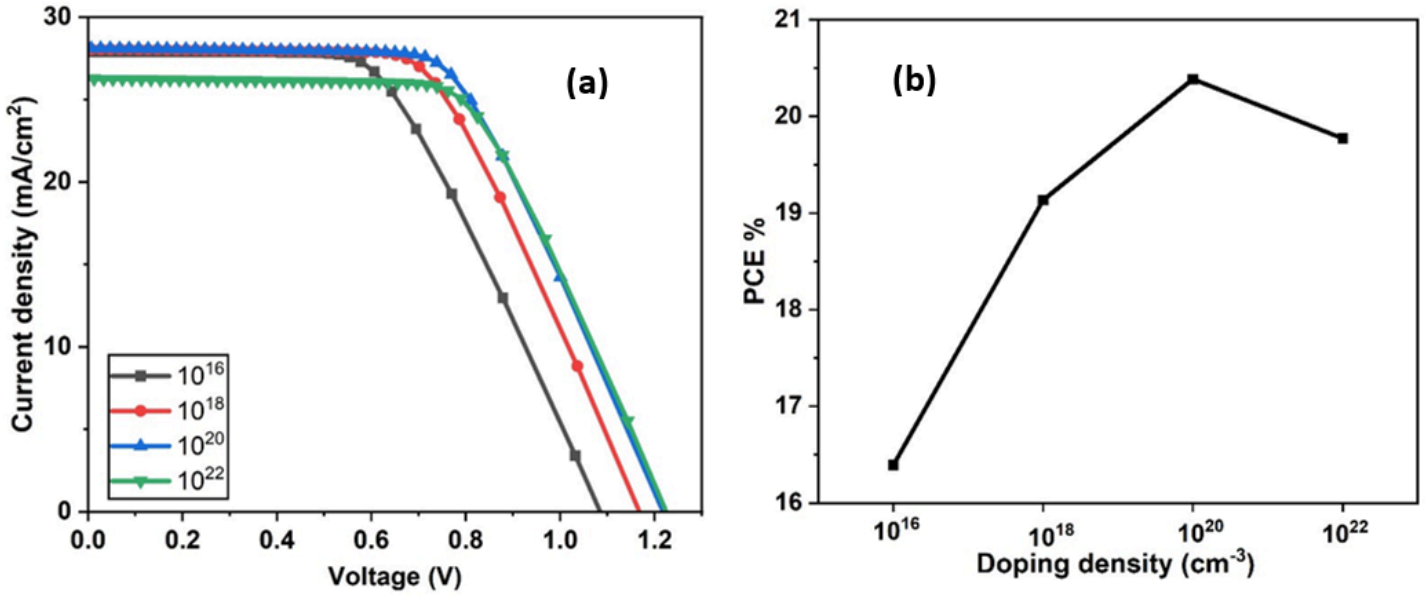

Figure 4

The simulation results of (FTO/CdS/Cs_2PtI_6 (600 nm)/Pt with different N_A concentration (a) J-V, (b) PCE

Supplementary Files

This is a list of supplementary files associated with this preprint. Click to download.

- suppcs2pti6htl.docx